Applied Surface Science 314 (2014) 931–935

Contents lists available at ScienceDirect

Applied Surface Science

journal homepage: www.elsevier.com/locate/apsusc

Excellent acetone sensing properties of Sm-doped α-Fe_2O_3

Chang Su [a], Changbai Liu [b], Li Liu [a,*], Mucui Ni [a], Haiying Li [a], Xiaoqing Bo [a], Lili Liu [a], Xiao Chi [a]

[a] State Key Laboratory of Superhard Materials, College of Physics, Jilin University, Changchun 130012, PR China
[b] College of Electronic Science & Engineering, Jilin University, Changchun 130012, PR China

ARTICLE INFO

Article history:
Received 21 January 2014
Received in revised form 18 June 2014
Accepted 29 June 2014
Available online 5 July 2014

Keywords:
Sm
α-Fe_2O_3 nanotubes
Acetone
Gas-sensing

ABSTRACT

Pure and 3 wt% Sm-doped α-Fe_2O_3 nanotubes are prepared via a typical electrospinning technology and calcination procedure. The characteristic and morphology of the synthesized nanotubes are investigated by X-ray diffraction (XRD), X-ray photoelectron spectroscopy (XPS) and scanning electron microscope (SEM). Compared with pure α-Fe_2O_3 nanotubes, 3 wt% Sm-doped α-Fe_2O_3 nanotubes display enhanced gas-sensing properties. The response of 3 wt% Sm-doped α-Fe_2O_3 nanotubes is 33–50 ppm acetone, which is 13 times larger than that of pure α-Fe_2O_3 nanotubes. The lowest detection limit of acetone is 500 ppb to which the response is 2.3 at the optimum operating temperature of 240 °C. The response and recovery times are about 6 and 11 s to 50 ppm acetone, respectively. In addition, 3 wt% Sm-doped α-Fe_2O_3 nanotubes exhibit good selectivity and long term stability.

1. Introduction

Semiconductor oxides have been widely studied and used all over the world, due to their applications in lithium storage [1,2], catalyst [3], photosensitization [4,5] and gas sensor [6,7]. Especially in the field of gas sensor, semiconductor oxides, as the gas sensing materials, have been playing an increasingly important role in people's life, which has drawn more attentions in order to obtain the new materials with the better gas sensing properties. Therefore, there are some drawbacks of semiconductor oxides that have to be overcome, like low response, high working temperature, bad selectivity and poor long-term stability. For now, much work has been done to solve these problems, among which the most effective method is synthesizing the composite materials. For instance, TiO_2/ZnO_2 nanocomposites have been successfully prepared, and it has been proved that the TiO_2/ZnO_2 nanocomposites possess the higher response to ethanol than ZnO_2 or TiO_2 nanomaterials [8]. The sensor based on Pd^0-Loaded SnO_2 nanofibers shows ultrasensitivity to H_2 at room temperature [9].

α-Fe_2O_3 is an n-type semiconductor, which has been widely used as the gas sensing materials to fabricate the gas sensor, due to its good long-term stability in the atmospheric condition, low cost and most easy availability. Rare earth elements have been extensively studied over the past decades due to their particular characteristics [10,11]. A lot of work has proved that doping rare earth element is a good way to enhance the gas-sensing properties of materials [12,13]. As one of the rare earth elements, Sm is also used for improving the gas-sensing properties of materials [14,15]. However, there is rare work to research the effect on the sensing properties of α-Fe_2O_3 nanotubes by doping Sm. In this paper, pure and Sm-doped α-Fe_2O_3 nanotubes are successfully obtained via the single nozzle electrospinning and calcination method. Furthermore, the gas-sensing properties of the as-synthesized materials to acetone are also investigated. The results demonstrate that the gas-sensing properties of α-Fe_2O_3 nanotubes have been enhanced significantly by doping Sm.

2. Experimental

2.1. Materials

All the chemistry reagents were analytical grade and used without further purification. Poly(vinyl pyrrolidone) (PVP, Mw = 1,300,000) was obtained from Sigma–Aldrich (USA). $Fe(NO_3)_3 \cdot 9H_2O$ (99.99%), $Sm(NO_3)_3 \cdot 6H_2O$ (99.99%), N,N-dimethylformamide (DMF, ≥99.5%) and ethanol (≥99.7%) were purchased from Aladdin (China).

2.2. Synthesis of pure and Sm-doped nanotubes

At first, 5.5 g ethanol and 0.55 g PVP were mixed. Meantime, 2.1 g DMF was mixed with 0.49 g $Fe(NO_3)_3 \cdot 9H_2O$ and $Sm(NO_3)_3 \cdot 6H_2O$ (in

* Corresponding author. Tel.: +86 431 8502260; fax: +86 431 8502260.
E-mail addresses: liul99@jlu.edu.cn, liuli_teacher@163.com (L. Liu).

http://dx.doi.org/10.1016/j.apsusc.2014.06.169
0169-4332/

a ratio of 0%, 1%, 3% and 5%). The two mixtures were under vigorous stirring for 2 h. Then, the two solutions were mixed and then stirred for 8 h. At last, the solution was injected from a single stainless steel capillary with a voltage of 13 kV. The distance between stainless steel capillary and non-woven mats collector was 20 cm. Subsequently, the collected composite fibers were calcined at 550 °C for 4 h and the pure and Sm-doped nanotubes were obtained.

2.3. Characterization

A PANalytical B.V. Empyrean X-ray diffraction (XRD) with Cu Kα1 radiation (λ = 1.5418 Å) was employed to analyze structure characterization. Scanning electron microscope (SEM) images were performed on a FEI XL30 instrument. The sensing properties of the sensor were measured by a CGS-8 intelligent gas-sensing analysis system (Beijing Elite Tech Co., Ltd., China).

2.4. Fabrication of gas sensor

The process of gas sensor fabrication is described in the previous work [16]. In details, the samples were added in an amount of deionized water to form slurry. Subsequently, the slurry was coated on a ceramic tube on which a pair of gold electrodes was previously printed. A spring-like Ni–Cr was plugged in the ceramic tube to provide the operating temperature. The gas sensor was dried for 5 days before the first measurement.

The sensor response ($S = R_a/R_g$) was defined as the ratio of the sensor resistances in the air (R_a) and in the target gas (R_g). The time taken by the sensor to achieve 90% of the resistance variation was response time, and when the sensor was opened to the air the time taken to return 90% of the resistance variation was recovery time.

3. Results and discussion

3.1. Structure and morphological characteristics

The XRD pattern of 3 wt% Sm-doped Fe_2O_3 nanotubes is showed in Fig. 1. The peaks are matched to hematite (JCPDS: 39-1346). Another peak (14-2) is observed, which is part of the spectra of Sm^{3+}, through which the formation of Fe_2O_3 and Sm_2O_3 can be evidenced. Further evidence for the formations of Fe_2O_3 and Sm_2O_3 can be researched by XPS, and the results are showed in Fig. 2. Fig. 2A shows the spectrum of Fe 2p, in which the two peaks at 711 and 724.8 eV correspond to Fe $2p_{3/2}$ and Fe $2p_{1/2}$, respectively [17]. Moreover, Fig. 2B reveals the two peaks at binding energy of

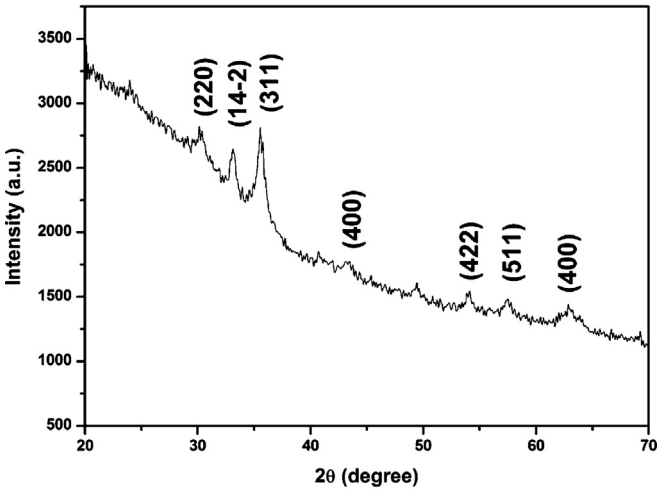

Fig. 1. XRD pattern of 3 wt% Sm-doped α-Fe_2O_3 nanotubes.

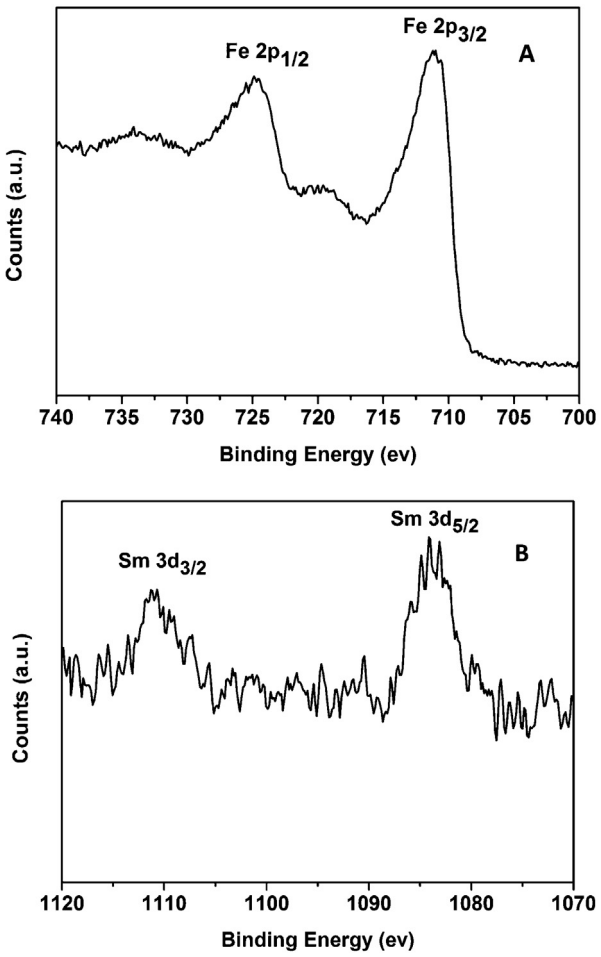

Fig. 2. XPS spectra of (A) Fe 2p and (B) Sm 3d of the as-prepared Sm-doped Fe_2O_3 nanotubes.

1084 and 111.3 eV, which correspond to Sm $3d_{5/2}$ and Sm $3d_{3/2}$ in Sm_2O_3 [18]. SEM images of pure and 3 wt% Sm-doped α-Fe_2O_3 nanotubes calcined at 550 °C are presented in Fig. 3. As is shown in Fig. 3(A), the average diameter of pure α-Fe_2O_3 nanotubes is about 90 nm. And the diameter of 3 wt% Sm-doped α-Fe_2O_3 nanotubes is basically unchanged which is evidenced by Fig. 3(B) and (C).

3.2. Gas-sensing properties

The sensors are tested at different operating temperatures in order to find the optimum operating temperature. Fig. 4 shows the relationship between the response and operating temperature to 50 ppm acetone. It can be seen that the responses of all α-Fe_2O_3 nanotubes sensors increase to the highest value at 240 °C and decrease rapidly with the operating temperature increasing. So, 240 °C is defined as optimum operating temperature. All the Sm-doped α-Fe_2O_3 nanotubes sensors show a better response than pure α-Fe_2O_3 nanotubes sensors, and 3 wt% Sm-doped α-Fe_2O_3 nanotubes sensors show the best response, which is 33 about 13 times larger than pure α-Fe_2O_3 nanotubes sensors (2.5) to 50 ppm acetone at 240 °C. The gas-sensing property of α-Fe_2O_3 nanotubes is remarkably enhanced by doping Sm. The perfect gas-sensing property makes it potentially qualified to be used for gas sensor.

The response and recovery times are important factors to assess the gas-sensing properties of sensors. Fig. 5 depicts the response and recovery curves of pure and 3 wt% Sm-doped α-Fe_2O_3 nanotubes sensors to 50 ppm acetone at 240 °C. It can be observed that the response and recovery times change slightly. The response and

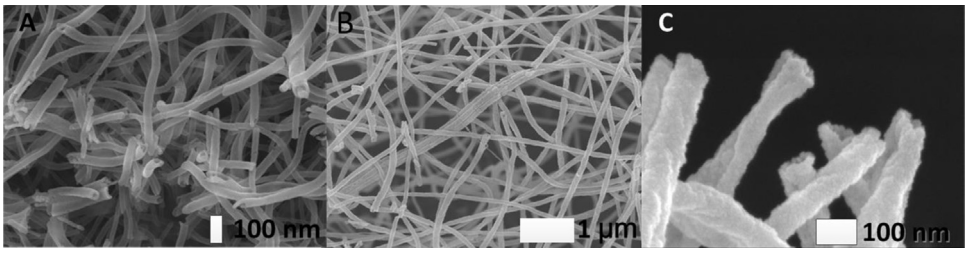

Fig. 3. SEM images of (A) pure α-Fe_2O_3 nanotubes, and (B, C) low and high-magnification of 3 wt% Sm-doped α-Fe_2O_3 nanotubes, respectively.

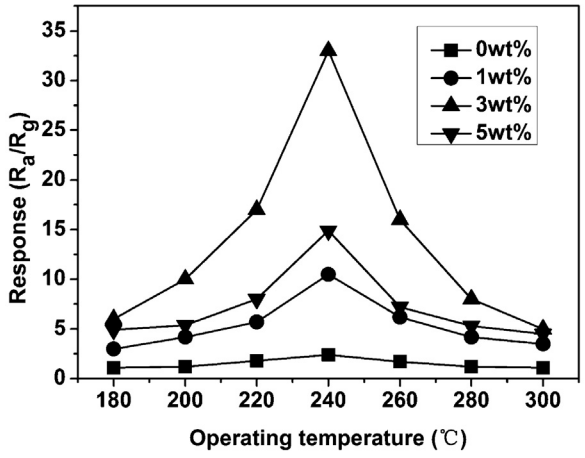

Fig. 4. Response curves of pure, 1 wt%, 3 wt% and 5 wt% Sm-doped α-Fe_2O_3 nanotubes sensors at different operating temperature to 50 ppm acetone.

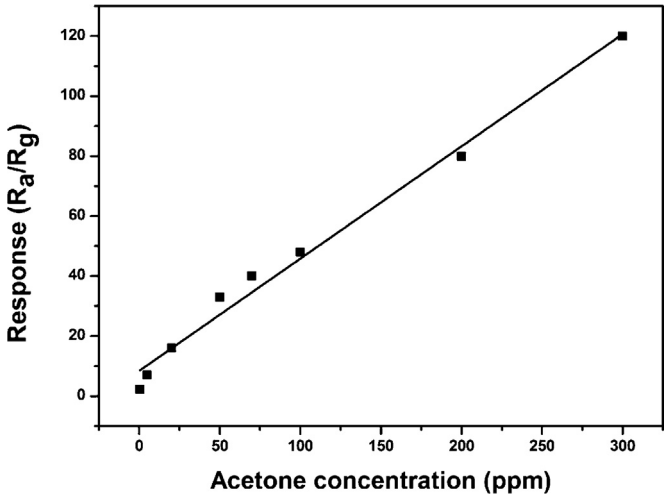

Fig. 6. The response curve of 3 wt% Sm-doped α-Fe_2O_3 nanotubes sensor at 240 °C to different acetone concentration.

recovery times of 3 wt% Sm-doped α-Fe_2O_3 nanotubes sensors are 6 and 11 s, respectively to 50 ppm acetone at 240 °C.

The experiment of testing the response of 3 wt% Sm-doped α-Fe_2O_3 nanotubes sensors to different acetone concentration at 240 °C is showed by Fig. 6 (Table 1). It displays that the response changes linearly between 0.5 and 300 ppm. The most important aspect of gas-sensing properties is the lowest detection limit concentration. The 3 wt% Sm-doped α-Fe_2O_3 nanotubes sensors can detect 0.5 ppm acetone and the response is 2.3. So, the 3 wt% Sm-doped α-Fe_2O_3 nanotubes can be used to fabricate gas sensor.

The selective test is described in Fig. 7. The sensing properties of 3 wt% Sm-doped α-Fe_2O_3 nanotubes sensors to 20, 50, 100 ppm acetone, formaldehyde, toluene, ammonia, hydrogen and butane are measured at 240 °C. It appears less sensitive to formaldehyde, toluene, ammonia, hydrogen and butane, and much better to acetone. These confirm that 3 wt% Sm-doped α-Fe_2O_3 nanotubes sensors display a good selective ability to acetone.

Long-term stability of 3 wt% Sm-doped α-Fe_2O_3 nanotubes sensors (20, 50 and 100 ppm acetone) is showed in Fig. 8. The sensors are tested every 15 days. The sensors display a good long-term stability, due to the character of Fe_2O_3. This character indicates the Sm-doped α-Fe_2O_3 nanotubes sensor can be used in practical application.

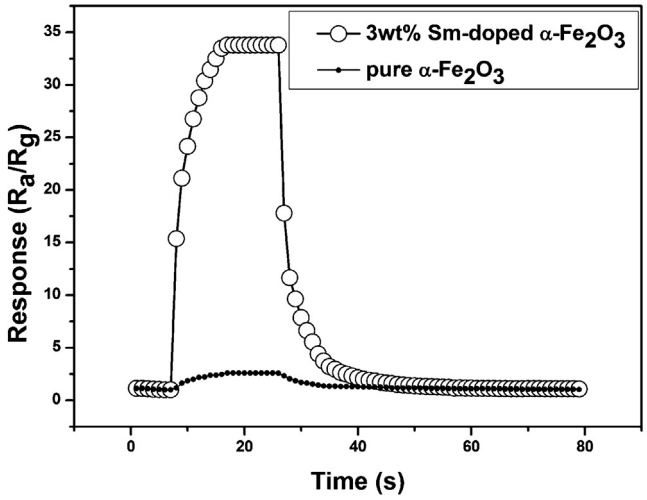

Fig. 5. Response–recovery curves of pure and 3 wt% Sm-doped α-Fe_2O_3 nanotubes sensors at 240 °C to 50 ppm acetone.

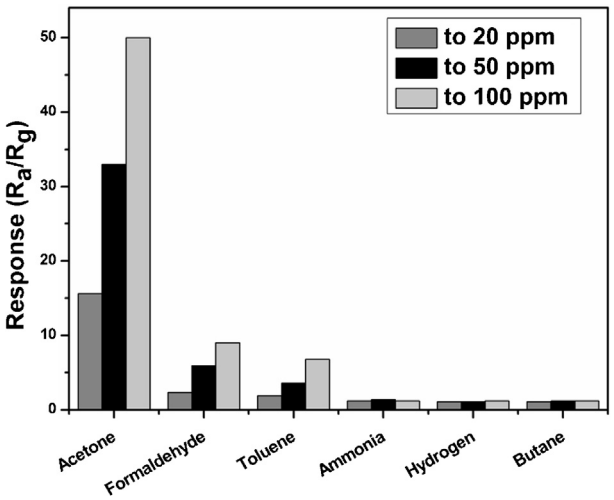

Fig. 7. The responses of 3 wt% Sm-doped α-Fe_2O_3 nanotubes sensor to 20, 50, 100 ppm different gas at 240 °C.

Table 1
Comparison between sensors based on Sm-doped α-Fe_2O_3 nanotubes and other acetone gas sensors.

Gas sensor	Definition of sensitivity	Operating temperature (°C)	Acetone concentration (ppm)	Value of sensitivity (about)	Reference
Sm-doped α-Fe_2O_3	Ra/Rg	240	50	33	This work
α-Fe_2O_3/SnO_2	Ra/Rg	250	100	16.8	[19]
CuO/α-Fe_2O_3	Ra/Rg	380	100	19.2	[20]
α-Fe_2O_3	Ra/Rg	270	50	9.0	[21]
α-Fe_2O_3	Ra/Rg	240	500	3.8	[22]

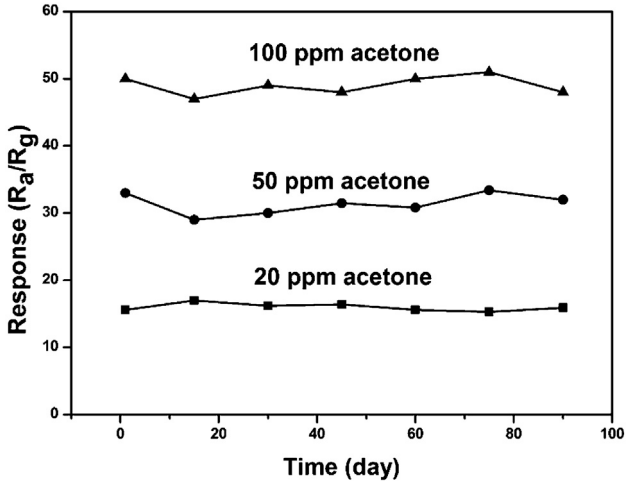

Fig. 8. The responses of 3 wt% Sm-doped α-Fe_2O_3 nanotubes sensor is measured every 15 days at 240 °C.

α-Fe_2O_3 is an n-type semiconductor, and the most accepted gas sensing mechanism is the change of the sensor resistance caused by the chemisorbed oxygen species on the surface of Fe_2O_3. When the sensor is exposed to air, the O_2 will turn to O_2^-, O^- and O^{2-} due to reaction with e^-. As result, the conductivity of Fe_2O_3 declines. And when the sensor is exposed to a target gas, like acetone, acetone will react with oxygen species (O_2^-, O^- and O^{2-}) and form CO_2 and H_2O. And the electronic is released to improve the conductivity of Fe_2O_3 at the same time. Thus the resistance change of Fe_2O_3 is formed [21]. As the formulas describe:

$$O_2 + e^- \leftrightarrow O_2^-, O^-, O^{2-} \quad (1)$$

$$C_3H_6O + O_2^-, O^-, O^{2-} \leftrightarrow CO_2 + H_2O + e^- \quad (2)$$

The unique nanotubes structure is beneficial to enhance the sensing properties. On one hand, the nanotubes structure is an ultrahigh surface-to-volume ratios structure that can adsorb more oxygen species than nanofibers and nanoparticles [23]. On the other hand, nanotube structure can facilitate full and fast access to improve the rate of transporting electronic or negative charged to the surface of Fe_2O_3 [24].

Sm-doped α-Fe_2O_3 nanotubes sensors exhibit better sensitivity than pure α-Fe_2O_3 nanotubes sensors. That can be explained as follows. More oxygen species will be adsorbed due to the addition of Sm. Thereby, the reaction between oxygen species and target gas becomes more violent when the sensor is exposed to the target gas [14,25]. As result, the resistance variation changes in a larger scale. These increase the sensitive. However, higher concentration Sm-doped makes the sensing response decrease, since it makes the decrease of the effective surface adsorption areas [26,27].

4. Conclusion

In summary, pure and Sm-doped nanotubes are prepared via electrospinning and following calcined procedure. Gas sensing properties investigation evidences that Sm-doped can enhance the acetone sensing properties of α-Fe_2O_3 nanotubes sensor remarkably. The response of 3 wt% Sm-doped α-Fe_2O_3 nanotubes sensor is 33 at 240 °C to 50 ppm acetone, which is 13 times larger than that of pure α-Fe_2O_3 nanotubes sensor, and the response and recovery times are 6 and 11 s, respectively. Moreover, the 3 wt% Sm-doped α-Fe_2O_3 nanotubes sensor possesses a good selectivity to acetone, low detection concentration (500 ppb) and long-term stabilities. These advantages make Sm-doped α-Fe_2O_3 nanotubes potentially qualified to fabricate high performance acetone sensor in practically.

Acknowledgments

The work has been supported by Jilin Provincial Science and Technology Department (20140204027GX), competition funded projects of “challenge cup” college students’ extracurricular academic science and technology works (201311).

References

[1] A. Brandt, A. Balducci, Ferrocene as precursor for carbon-coated α-Fe_2O_3 nanoparticles for rechargeable lithium batteries, J. Power Sources 230 (2013) 44–49.
[2] Y. Xiao, C. Hu, M. Cao, High lithium storage capacity and rate capability achieved by mesoporous Co_3O_4 hierarchical nanobundles, J. Power Sources 247 (2014) 49–56.
[3] I.V. Lightcap, T.H. Kosel, P.V. Kamat, Anchoring semiconductor and metal nanoparticles on a two-dimensional catalyst mat. storing and shuttling electrons with reduced graphene oxide, Nano Lett. 10 (2010) 577–583.
[4] P. Kar, T. Banerjee, S. Verma, A. Sen, A. Das, B. Ganguly, H.N. Ghosh, Photosensitization of nanoparticulate TiO2 using a Re(i)-polypyridyl complex: studies on interfacial electron transfer in the ultrafast time domain, Phys. Chem. Chem. Phys. 14 (2012) 8192.
[5] K.S. Leschkies, R. Divakar, J. Basu, E. Enache-Pommer, J.E. Boercker, C.B. Carter, U.R. Kortshagen, D.J. Norris, E.S. Aydil, Photosensitization of ZnO nanowires with CdSe quantum dots for photovoltaic devices, Nano Lett. 7 (2007) 1793–1798.
[6] A. Gurlo, Nanosensors: towards morphological control of gas sensing activity. SnO2, In2O3, ZnO and WO3 case studies, Nanoscale 3 (2011) 154.
[7] W. Zheng, Z. Li, H. Zhang, W. Wang, Y. Wang, C. Wang, Electrospinning route for α-Fe_2O_3 ceramic nanofibers and their gas sensing properties, Mater. Res. Bull. 44 (2009) 1432–1436.
[8] Z. Lou, J. Deng, L. Wang, R. Wang, T. Fei, T. Zhang, A class of hierarchical nanostructures: ZnO surface-functionalized TiO_2 with enhanced sensing properties, RSC Adv. 3 (2013) 3131.
[9] Z. Wang, Z. Li, T. Jiang, X. Xu, C. Wang, Ultrasensitive hydrogen sensor based on Pd0-loaded SnO_2 electrospun nanofibers at room temperature, ACS Appl. Mater. Interfaces 5 (2013) 2013–2021.
[10] L. Xu, B. Dong, Y. Wang, X. Bai, J. Chen, Q. Liu, H. Song, Porous In2O3: RE (RE = Gd, Tb, Dy, Ho, Er, Tm, Yb) nanotubes: electrospinning preparation and room gas-sensing properties, J. Phys. Chem. C 114 (2010) 9089–9095.
[11] H. Aono, E. Traversa, M. Sakamoto, Y. Sadaoka, Crystallographic characterization and NO2 gas sensing property of LnFeO3 prepared by thermal decomposition of Ln·Fe hexacyanocomplexes, $Ln[Fe(CN)_6]\cdot nH_2O$, Ln = La, Nd, Sm, Gd, and Dy, Sens. Actuators B: Chem. 94 (2003) 132–139.
[12] W. Qin, L. Xu, J. Song, R. Xing, H. Song, Highly enhanced gas sensing properties of porous SnO2–CeO2 composite nanofibers prepared by electrospinning, Sens. Actuators B: Chem. 185 (2013) 231–237.
[13] Y. Liu, Y. Ding, H. Gao, L. Zhang, P. Gao, B. Li, Y. Lei, La0.67Sr0.33MnO3 nanofibers for in situ, real-time, and stable high temperature oxygen sensing, RSC Adv. 2 (2012) 3872.
[14] M.M. Rahman, A. Jamal, S.B. Khan, M. Faisal, Fabrication of highly sensitive ethanol chemical sensor based on Sm-doped Co3O4 nanokernels by a hydrothermal method, J. Phys. Chem. C 115 (2011) 9503–9510.
[15] S. Gupta, S.V.N.T. Kuchibhatla, M.H. Engelhard, V. Shutthanandan, P. Nachimuthu, W. Jiang, L.V. Saraf, S. Thevuthasan, S. Prasad, Influence of samaria doping on the resistance of ceria thin films and its implications to the planar oxygen sensing devices, Sens. Actuators B: Chem. 139 (2009) 380–386.

[16] L. Liu, C. Liu, S. Li, L. Wang, H. Shan, X. Zhang, H. Guan, Z. Liu, Honeycombed SnO2 with ultra sensitive properties to H_2, Sens. Actuators B: Chem. 177 (2013) 893–897.
[17] H. Shan, C. Liu, L. Liu, J. Zhang, H. Li, Z. Liu, X. Zhang, X. Bo, X. Chi, Excellent toluene sensing properties of SnO2–Fe2O3 interconnected nanotubes, ACS Appl. Mater. Interfaces 5 (2013) 6376–6380.
[18] M. Mo, K.S. Hui, X. Hong, J. Guo, C. Ye, A. Li, N. Hu, Z. Huang, J. Jiang, J. Liang, H. Chen, Improved cycling and rate performance of Sm-doped LiNi0.5Mn1.5O4 cathode materials for 5 V lithium ion batteries, Appl. Surf. Sci. 290 (2014) 412–418.
[19] P. Sun, Y. Cai, S. Du, X. Xu, L. You, J. Ma, F. Liu, X. Liang, Y. Sun, G. Lu, Hierarchical α-Fe_2O_3/SnO_2 semiconductor composites: hydrothermal synthesis and gas sensing properties, Sens. Actuators B: Chem. 182 (2013) 336–343.
[20] Y. Kang, L. Wang, Y. Wang, H. Zhang, Y. Wang, D. Hong, Y. Qv, S. Wang, Construction and enhanced gas sensing performances of CuO-modified α-Fe2O3 hybrid hollow spheres, Sens. Actuators B: Chem. 177 (2013) 570–576.
[21] J. Ma, J. Teo, L. Mei, Z. Zhong, Q. Li, T. Wang, X. Duan, J. Lian, W. Zheng, Porous platelike hematite mesocrystals: synthesis, catalytic and gas-sensing applications, J. Mater. Chem. 22 (2012) 11694.
[22] H. Shan, C. Liu, L. Liu, L. Wang, S. Li, X. Zhang, X. Bo, X. Chi, Synthesis and acetone gas sensing properties of α-Fe2O3 nanotubes, Sci. China Chem. 56 (2013) 1722–1726.
[23] N. Du, H. Zhang, B.D. Chen, X.Y. Ma, Z.H. Liu, J.B. Wu, D.R. Yang, Porous indium oxide nanotubes: layer-by-layer assembly on carbon-nanotube templates and application for room-temperature NH3 gas sensors, Adv. Mater. 19 (2007) 1641–1645.
[24] X. Chen, Z. Guo, W.-H. Xu, H.-B. Yao, M.-Q. Li, J.-H. Liu, X.-J. Huang, S.-H. Yu, Templating synthesis of SnO2 nanotubes loaded with Ag2O nanoparticles and their enhanced gas sensing properties, Adv. Funct. Mater. 21 (2011) 2049–2056.
[25] H.T. Giang, H.T. Duy, P.Q. Ngan, G.H. Thai, D.T.A. Thu, D.T. Thu, N.N. Toan, High sensitivity and selectivity of mixed potential sensor based on Pt/YSZ/SmFeO3 to NO2 gas, Sens. Actuators B: Chem. 183 (2013) 550–555.
[26] C. Ge, C. Xie, M. Hu, Y. Gui, Z. Bai, D. Zeng, Structural characteristics and UV-light enhanced gas sensitivity of La-doped ZnO nanoparticles, Mater. Sci. Eng. B 141 (2007) 43–48.
[27] H. Shan, C. Liu, L. Liu, S. Li, L. Wang, X. Zhang, X. Bo, X. Chi, Highly sensitive acetone sensors based on La-doped α-Fe2O3 nanotubes, Sens. Actuators B: Chem. 184 (2013) 243–247.